Reinvestigation of the dysbindin subunit of BLOC-1 (biogenesis of lysosome-related organelles complex-1) as a dystrobrevin-binding protein

Ramin NAZARIAN*, Marta STARCEVIC*, Melissa J. SPENCER†‡ and Esteban C. DELL'ANGELICA*[1]

*Department of Human Genetics, David Geffen School of Medicine, University of California, Los Angeles, CA 90095, U.S.A., †Departments of Neurology and Pediatrics, David Geffen School of Medicine, University of California, Los Angeles, CA 90095, U.S.A., and ‡Duchenne Muscular Dystrophy Research Center, University of California, Los Angeles, CA 90095, U.S.A.

Dysbindin was identified as a dystrobrevin-binding protein potentially involved in the pathogenesis of muscular dystrophy. Subsequently, genetic studies have implicated variants of the human dysbindin-encoding gene, *DTNBP1*, in the pathogeneses of Hermansky–Pudlak syndrome and schizophrenia. The protein is a stable component of a multisubunit complex termed BLOC-1 (biogenesis of lysosome-related organelles complex-1). In the present study, the significance of the dystrobrevin–dysbindin interaction for BLOC-1 function was examined. Yeast two-hybrid analyses, and binding assays using recombinant proteins, demonstrated direct interaction involving coiled-coil-forming regions in both dysbindin and the dystrobrevins. However, recombinant proteins bearing the coiled-coil-forming regions of the dystrobrevins failed to bind endogenous BLOC-1 from HeLa cells or mouse brain or muscle, under conditions in which they bound the Dp71 isoform of dystrophin. Immunoprecipitation of endogenous dysbindin from brain or muscle resulted in robust co-immunoprecipitation of the pallidin subunit of BLOC-1 but no specific co-immunoprecipitation of dystrobrevin isoforms. Within BLOC-1, dysbindin is engaged in interactions with three other subunits, named pallidin, snapin and muted. We herein provide evidence that the same 69-residue region of dysbindin that is sufficient for dystrobrevin binding *in vitro* also contains the binding sites for pallidin and snapin, and at least part of the muted-binding interface. Functional, histological and immunohistochemical analyses failed to detect any sign of muscle pathology in BLOC-1-deficient, homozygous pallid mice. Taken together, these results suggest that dysbindin assembled into BLOC-1 is not a physiological binding partner of the dystrobrevins, likely due to engagement of its dystrobrevin-binding region in interactions with other subunits.

Key words: biogenesis of lysosome-related organelles complex-1 (BLOC-1), dysbindin, dystrobrevin, Hermansky–Pudlak syndrome (HPS), muscular dystrophy, schizophrenia.

INTRODUCTION

The α- and β-dystrobrevins are closely related proteins that display significant homology to, and interact with, dystrophin, which is the product of the gene deficient in Duchenne and Becker muscular dystrophies [1,2]. Dystrophin is a key component of the DGC (dystrophin–glycoprotein complex), also known as dystrophin-associated protein complex, which directly links the intracellular cytoskeleton to the extracellular matrix and serves as a scaffold for proteins involved in signal transduction [1–3]. The α- and β-dystrobrevins are the products of two distinct genes, and comprise several isoforms generated by alternative splicing or the use of alternative promoters [1,2]. Various isoforms of α-dystrobrevin are expressed mainly (but not exclusively) in fully differentiated myotubes, where they exist as components of the DGC at the sarcolemma and the neuromuscular junction [4]. Consistent with such locations, mice deficient in α-dystrobrevin display muscular dystrophy and defective postsynaptic acetylcholine receptor clusters at the neuromuscular junction [5,6]. On the other hand, β-dystrobrevin is not detectable in adult muscle but it is expressed in brain, liver and kidney, where it associates with dystrophin isoforms into DGC-like complexes [7,8]. Mice deficient in β-dystrobrevin are apparently healthy but display reduced membrane-associated pools of two dystrophin isoforms, Dp71 and Dp71ΔC, in kidney and liver cells [9].

The dystrobrevins interact physically not only with dystrophin but also with the syntrophins, which are likewise components of the DGC and related complexes [1–3]. Additional dystrobrevin-interacting partners have been described [1,2,10,11], including a novel protein named dysbindin [12]. Human dysbindin is encoded by the *DTNBP1* gene, and its predicted amino acid sequence shares no significant identity with that of any protein of known function [12]. Interaction between mouse dysbindin and both α- and β-dystrobrevins was demonstrated using the yeast two-hybrid system and co-immunoprecipitation of binding partners overexpressed in transfected COS-7 cells [12,13]. Co-immunoprecipitation of endogenously expressed dysbindin, dystrobrevins and dystrophin isoforms from rat brain and muscle was also reported [12] and led to the notion that dysbindin may be a component of the DGC [4]. In support of the idea that dysbindin might be involved in the pathogenesis of muscular dystrophy, the protein was found at increased levels in muscle from dystrophin-deficient, mdx mutant mice [12].

Besides the proposed role of dysbindin in muscle physiology and disease, accumulating evidence argues for a role of dysbindin in the pathogenesis of schizophrenia, a common psychiatric disorder with significant, but complex, genetic involvement [14–16]. Specifically, haplotype variations in non-coding regions of the *DTNBP1* gene have been associated with a higher risk of developing the disease [14–16]. Furthermore, partial reductions

Abbreviations used: 3AT, 3-amino-1,2,4-triazole; BLOC, biogenesis of lysosome-related organelles complex; BLOS3, BLOC subunit 3; DGC, dystrophin–glycoprotein complex; GST, glutathione S-transferase; HPS, Hermansky–Pudlak syndrome; MYH9, non-muscle myosin heavy polypeptide 9; ORF, open reading frame; Rab6ip2, Rab6-interacting protein 2; RT, reverse transcriptase.

[1] To whom correspondence should be addressed (email Edellangelica@mednet.ucla.edu).

The nucleotide sequence of human β-dystrobrevin isoform 6 has been deposited in the DDBJ, EMBL, GenBank® and GSDB Nucleotide Sequence Databases under the accession number DQ160290.

in dysbindin mRNA [17,18] and protein [19] levels have been observed in post-mortem brain samples of schizophrenic patients. Consistent with a neuronal function for dysbindin, both its over-expression and down-regulation in cultured cortical neurons were found to affect pre-synaptic protein expression levels, glutamate exocytosis and Akt-dependent signalling [20].

Strikingly, evidence for the role of dysbindin in the pathogenesis of yet another genetic disease has been reported. The disease, named Hermansky–Pudlak syndrome (HPS), is characterized by defective biogenesis of cell-type-specific, lysosome-related organelles such as melanosomes and platelet dense granules [21–23]. Melanosome defects lead to oculocutaneous albinism, while defects in platelet dense granules result in prolonged bleeding times and bruising. Over a dozen mutant mouse strains, which arose by spontaneous mutations and display a similar combination of hypopigmentation and bleeding diathesis, serve as animal models of HPS [21]. One of these strains, named sandy, carries an in-frame deletion in the dysbindin-encoding gene [13]. Genetic and biochemical data demonstrated stable association of dysbindin into a widely expressed, multisubunit protein complex named BLOC-1 (biogenesis of lysosome-related organelles complex-1) [13,24]. Among other BLOC-1 subunits are the proteins pallidin, muted, cappuccino and BLOS3 (BLOC subunit 3), all of which are encoded by genes mutated in mouse strains that, like sandy, display HPS-like phenotypes [24–30]. Furthermore, a nonsense mutation in *DTNBP1* has been described in a patient suffering from the typical manifestations of HPS [13].

The potential significance of the dystrobrevin–dysbindin interaction for muscular dystrophy, schizophrenia and HPS prompted us to characterize it further, particularly in light of the recent demonstration that dysbindin is a subunit of BLOC-1 [13,24]. In the present study, we have found that binding of isolated dysbindin to the dystrobrevins involves coiled-coil-forming domains of both interacting partners. Unexpectedly, we have also obtained evidence suggesting that dysbindin assembled into native BLOC-1 is unable to bind dystrobrevins *in vivo*, probably due to engagement of its dystrobrevin-binding region in interaction with other subunits. We also report that the apparent increase in dysbindin protein levels in mdx muscle does not necessarily imply specific up-regulation of dysbindin protein expression, and that BLOC-1-deficient pallid mice display no detectable signs of muscle pathology. Together, these results argue against the notion that BLOC-1 is a physiological binding partner of the dystrobrevins.

EXPERIMENTAL

DNA constructs

All of the plasmids used in the present study consisted of human cDNA sequences that were cloned in-frame into the EcoRI–SalI sites of the following vectors: pGBT9 and pGAD424 (BD Biosciences Clontech) to generate fusions to the Gal4 DNA-binding and activation domains respectively, pGEX-5X-1 (Amersham Biosciences) to generate GST (glutathione S-transferase)-fusion proteins, and pET-30a(+) (EMD Biosciences Novagen) to generate polyhistidine-fusion proteins. Yeast two-hybrid plasmids encoding the complete ORFs (open reading frames) of human pallidin, muted, dysbindin, snapin, BLOS1, BLOS2 or BLOS3 fused to the Gal4 DNA-binding or activation domains have been described elsewhere [24,26]. The plasmid containing the ORF of human dysbindin (GenBank® accession number AY265460) in the pGAD424 vector [24] was used as a template for PCR-based engineering of the DNA segments encoding dysbindin amino acid residues 1–223 (N-t), 224–351 (C-t), 72–223 (Dcc), 72–140 (Dc1) and 141–223 (Dc2), which were then cloned into pGAD424. The DNA segment encoding the dysbindin Dcc fragment was then subcloned into pET-30a(+) to generate the His–Dysbin(Dcc)-fusion protein. The full-length ORF of human β-dystrobrevin (isoform 6; GenBank® accession number DQ160290) was amplified by RT (reverse transcriptase)–PCR of total RNA extracted from HeLa cells, and then cloned into pGBT9. The resulting plasmid was used as a template for PCR-based engineering of the segments comprising amino acid residues 1–359 (N-t), 360–602 (C-t) and 422–518 (CC), which were also cloned into pGBT9. The ORF of human dysbindin-related protein (GenBank® accession number AJ276469) was PCR-amplified from IMAGE consortium (integrated molecular analysis of genomes and their expression consortium) cDNA clone 5260150 (American Type Culture Collection) and cloned into pGAD424. The cDNA segments encoding the following protein fragments, herein referred to as CC regions or CC fragments, were amplified by RT–PCR of HeLa RNA and cloned into pGBT9: amino acid residues 461–554 of human α-dystrobrevin isoform 1 (NCBI accession number NP_001381), residues 3265–3354 of human utrophin (NCBI accession number NP_009055) and residues 721–802 of human kinesin heavy chain Kif5B (NCBI accession number NP_004512). The plasmid encoding the CC region of α-dystrobrevin was then used as a template for PCR-based engineering of the segments encoding residues 461–500 (H1 segment) and 501–554 (H2 segment), which were also cloned into pGBT9. The DNA segment encoding the CC fragment of dystrophin (residues 415–517 of human dystrophin Dp71a isoform; NCBI accession number NP_004008) was PCR-amplified from IMAGE consortium cDNA clone 6187420 and cloned into pGBT9, pGAD424 and pET-30(+). The DNA segments encoding the CC fragments of α-dystrobrevin, β-dystrobrevin and utrophin were subcloned into pGEX-5X-1 to generate the GST–α-DBN(CC), GST–β-DBN(CC) and GST–Utroph(CC) fusion proteins, as well as into pET-30a(+) to generate the His–α-DBN(CC), His–β-DBN(CC) and His–Utroph(CC) fusion proteins respectively. The cDNA segments encoding the following protein fragments, herein referred to as Dcc regions or Dcc fragments, were amplified by either RT–PCR from HeLa RNA or PCR from a HeLa cDNA library (BD Biosciences Clontech) and cloned into pGAD424: amino acid residues 605–728 of human restin isoform a (NCBI accession number NP_002947), residues 686–829 of human Rab6ip2 (Rab6-interacting protein 2) isoform ε (NCBI accession number NP_829884) and residues 863–978 of human MYH9 (non-muscle myosin heavy polypeptide 9; also known as non-muscle myosin heavy chain IIA) (NCBI accession number NP_002464). The DNA segment encoding the Dcc fragment of MYH9 was subcloned into pET-30(+) to generate the His–MYH9(Dcc)-fusion protein. All constructs were verified by DNA sequencing.

Antibodies

The rabbit polyclonal antibody to human dysbindin was described previously [24]. The mouse monoclonal antibody to pallidin was generated in collaboration with Zymed Laboratories (San Francisco, CA, U.S.A.), using recombinant forms of full-length human pallidin [26] both as immunogen and antigen for screening of hybridoma clones. The antibody specifically recognizes the pallidin protein from human, mouse, rat and bovine samples by immunoblotting, although it does not seem to recognize its cognate antigen by immunofluorescence. The following monoclonal antibodies were purchased from the vendors indicated in parentheses: anti-polyhistidine clone His-1, anti-γ-adaptin clone 100/3 and anti-dystrophin clone MANDRA1 (Sigma–Aldrich), anti-dystrobrevin clone 23, anti-clathrin heavy chain clone 23

and anti-Rab11 clone 47 (BD Transduction Laboratories), anti-CD11b clone M1/70 (BD Pharmingen), anti-neural cell adhesion molecule clone H28.123 (Chemicon) and anti-dystrophin clone NCL-DYS2 (Novocastra). The rabbit polyclonal antibody to laminin was obtained from Sigma–Aldrich. Conjugated secondary antibodies were obtained from Vector Laboratories. The sources of all other commercial antibodies are described elsewhere [26].

Yeast two-hybrid experiments

Yeast two-hybrid assays were performed by co-transformation of haploid *Saccharomyces cerevisiae* strain AH109 (BD Biosciences Clontech) with pGBT9- and pGAD424-derived plasmids, selection of double transformants on minimal medium lacking leucine and tryptophan, and subsequent spotting of aqueous cell suspensions on the same medium (as control) or minimal medium lacking leucine, tryptophan and histidine and containing 3AT (3-amino-1,2,4-triazole), as described previously [26].

Preparation of extracts from HeLa cells

The source and culture conditions of human HeLa cells were described elsewhere [31]. All biochemical procedures were performed at 0–4 °C. Cells grown on monolayers were rinsed briefly with ice-cold PBS, detached using a plastic cell scraper, and homogenized in 'Detergent-free buffer' (20 mM Tris/HCl, pH 7.4, 0.1 M KCl, 1 mM EDTA and 1 mM dithiothreitol) supplemented with protease inhibitor mixture [1 mM 4-(2-aminoethyl)benzenesulphonyl fluoride, 10 mg/l leupeptin, 5 mg/l aprotinin and 1 mg/l pepstatin A], by 15–20 passages through a 25-gauge needle. The crude homogenate was first centrifuged for 10 min at 500 ***g***, and the resulting supernatant was further centrifuged for 90 min at 120 000 ***g*** to obtain a cytosolic extract and a membrane pellet. The membrane pellet was solubilized in 'Triton X-100 buffer' [10 mM Hepes, pH 7.0, 0.3 M sucrose, 0.1 M NaCl, 3 mM $MgCl_2$, 1 mM EGTA, 1 mM dithiothreitol and 0.5 % (w/v) Triton X-100] supplemented with protease inhibitor mixture, and then cleared by centrifugation for 10 min at 15 000 ***g***. In some experiments, HeLa cells were homogenized in 'Tween 20 buffer' [10 mM Tris/HCl, pH 8.0, 0.15 M NaCl and 0.1 % (v/v) Tween 20] supplemented with protease inhibitor mixture, by successive passages through a 25-gauge needle, and then cleared by centrifugation for 10 min at 500 ***g*** followed by a second centrifugation for 90 min at 120 000 ***g***.

Preparation of extracts from mouse and rat tissues

Animals were euthanized according to procedures approved by the UCLA (University of California, Los Angeles, CA, U.S.A.) Chancellor's Animal Research Committee. To prepare tissue extracts for affinity-pulldown experiments, frozen whole brain or quadriceps from adult C57BL/6J mice were thawed on ice, minced, and then homogenized in Detergent-free buffer supplemented with protease inhibitor mixture, using a hand-held rotor homogenizer (BioSpec Products). The crude homogenates were centrifuged for 10 min at 500 ***g***, and the resulting supernatant was further centrifuged for 90 min at 120 000 ***g*** to yield soluble cytosolic extracts and membrane pellets. Muscle membrane pellets were solubilized in Triton X-100 buffer supplemented with protease inhibitor mixture. Owing to their relatively higher lipid content, brain membrane pellets were solubilized in a similar buffer containing 1–2 % instead of 0.5 % Triton X-100. The solubilized membrane extracts were cleared by centrifugation for 10 min at 15 000 ***g***.

For co-immunoprecipitation experiments, minced brain and quadriceps were homogenized in 'Co-immunoprecipitation buffer' (10 mM Hepes, pH 7.0, 0.3 M sucrose, 0.1 M NaCl, 3 mM $MgCl_2$ and 1 mM EGTA) supplemented with protease inhibitor mixture and 0.5, 1 or 2 % Triton X-100, using a glass homogenizer. The homogenates were cleared by centrifugation for 10 min at 15 000 ***g***. In one experiment, the homogenate was further centrifuged for 90 min at 120 000 ***g***.

For immunoblotting analysis of steady-state protein levels, freshly dissected brains (frontal lobe) and muscle (quadriceps) from 2-month-old wild-type (C57BL/6J) and dystrophin-deficient (Dmd^{mdx}) male mice were minced and homogenized in 50 mM Tris/HCl (pH 7.5), 1 % Triton X-100, 0.25 % (w/v) sodium deoxycholate, 0.1 % (w/v) SDS, 0.15 M NaCl, 1 mM EDTA and protease inhibitor mixture, first by using a homogenizer with a plastic pestle and then by brief (20 s) sonication. The extracts were cleared by centrifugation for 5 min at 15 000 ***g***. Total protein concentration in the cleared extracts was estimated by Bradford's method [31a] using a commercial reagent (Bio-Rad) and BSA as the standard.

Affinity-'pulldown' binding experiments

Expression and affinity purification of GST- and polyhistidine-fusion proteins were performed as previously described [26]. GST-fusion proteins were immobilized on to 15 μl of glutathione–Sepharose 4 Fast Flow beads (Amersham Biosciences), and then incubated with purified polyhistidine-fusion proteins or cleared extracts prepared from HeLa cells or mouse tissues, in 1 ml of binding buffer (Detergent-free buffer, Triton X-100 buffer or Tween 20 buffer, as indicated). The amounts of GST-fusion protein used per sample were 5, 20 and 50 μg for incubations with polyhistidine fusion proteins, HeLa extracts and mouse tissue extracts respectively. In another set of experiments, polyhistidine-fusion proteins (25 μg) were immobilized on to 15 μl of Protein S–agarose beads (EMD Biosciences Novagen) and then incubated with cleared extracts from HeLa cells or mouse brain. In all cases, incubations were carried out for 1 h at 4 °C. Subsequently, beads were isolated by brief centrifugation and washed four times with 1 ml of ice-cold binding buffer, except for experiments using membranes solubilized in Triton X-100 buffer, where beads were first washed four times with a buffer containing 0.1 % Triton X-100 and then once with the same buffer without the detergent. Washed beads were heated to 95 °C upon addition of 15 μl of 2× SDS/PAGE sample buffer (0.1 M Tris/HCl, pH 6.8, 0.2 M dithiothreitol, 24 %, w/v, glycerol, 8 % SDS and 0.1 %, w/v, Bromophenol Blue) (Laemmli) [31b], and the eluted proteins were subsequently analysed by SDS/PAGE and immunoblotting.

Co-immunoprecipitation

Whole-tissue homogenates freshly prepared from mouse and rat tissues (brain or quadriceps muscle), using Co-immunoprecipitation buffer (10 mM Hepes, pH 7.0, 0.3 M sucrose, 0.1 M NaCl, 3 mM $MgCl_2$ and 1 mM EGTA) supplemented with protease inhibitors and Triton X-100 (0.5–2 % as indicated), were incubated with Protein G–Sepharose 4 Fast Flow beads and/or Protein A–Sepharose 4 Fast Flow beads (Amersham Biosciences) to remove endogenous IgG. Following a brief centrifugation, the cleared homogenates were divided into aliquots and incubated for 1 h at 4 °C with 2 μg of either anti-dystrobrevin mouse monoclonal antibody or irrelevant mouse IgG prebound to 15 μl of Protein G–Sepharose 4 Fast Flow beads, and with 2 μg of irrelevant rabbit IgG or affinity-purified rabbit antibodies to either dysbindin [24], GST or the ε subunit of the AP-4 complex [32] prebound to 15 μl of Protein A–Sepharose 4 Fast Flow beads. Following the incubation period, beads were isolated by brief

centrifugation and washed four times with 1 ml of Co-immunoprecipitation buffer containing 0.1 % Triton X-100. Washed beads were heated to 95 °C in the presence of 15 μl of 2× SDS/PAGE sample buffer, and the proteins eluted from the beads were analysed by SDS/PAGE followed by immunoblotting.

Immunoblotting

Proteins were fractionated on a pre-cast 4–20 % gradient SDS/polyacrylamide gel (Laemmli system; Invitrogen) and transferred by electroblotting to PVDF membranes. Membranes were incubated for at least 3 h with blocking buffer (PBS containing 5 %, w/v, non-fat milk and 2 % Tween 20) and sequentially with primary antibody (for 1 h) and horseradish peroxidase-conjugated secondary antibody (for 30 min), both of them diluted in blocking buffer. After incubation with each antibody, membranes were washed four times with PBS. Bound antibodies were detected by using ECL® or ECL$^+$ detection systems (Amersham Biosciences).

Analysis of muscle pathology in mice

Control (C57BL/6J) and pallid (*Pldn*^{pa}) mice of both genders and 4 months and 1 year of age were analysed following procedures approved by the institutional animal research committee. To assess strength, mice were allowed to freely grip a wire suspended 3 feet above ground and made to hang for five 1 min intervals [33]. To assess muscle histopathology, three muscles dissected from killed animals (quadriceps, gastrocnemius and tibialis anterior) were analysed. Muscles were embedded in Tissue-Tek® OCT Compound (Electron Microscopy Sciences) and quick-frozen in isopentane that had been precooled in liquid nitrogen. Cryosections of 10 μm-thickness were taken from each muscle and placed on gelatin-coated slides. For histological analysis, slides were stained with haematoxylin and visualized under a light microscope. Immunohistochemical staining for CD11b and anti-neural cell adhesion molecule was carried out to detect areas of muscle necrosis/inflammation and regeneration respectively. Additional immunostaining of unfixed sections (with anti-dystrophin antibody NCL-DYS2 followed by Texas Red-conjugated anti-mouse IgG), or sections that had been fixed with 2 % (w/v) paraformaldehyde (with anti-dystrobrevin or anti-laminin followed by appropriate fluorescein-conjugated secondary antibody), was carried out essentially as described elsewhere [34]. Binding of secondary anti-mouse IgG antibodies to endogenous IgG was blocked by using the MOM kit (Vector Laboratories).

RESULTS

Yeast two-hybrid analyses of the dystrobrevin–dysbindin interaction

We first examined the ability of full-length human β-dystrobrevin to bind dysbindin and related human proteins in the context of the yeast two-hybrid system, using haploid yeast cells co-transformed with plasmids encoding hybrids of these proteins with the DNA-binding and activation domains of the Gal4 transcription factor. In agreement with published results on the yeast-two hybrid interaction between mouse β-dystrobrevin and dysbindin [12,13], interaction between the human counterparts was robust, as evidenced by growth of co-transformed yeast cells on minimal medium lacking histidine and containing 5 mM 3AT (Figure 1A; 3AT inhibits the growth of cells expressing low levels of the *His3* reporter gene) as well as on medium lacking adenine (to test for expression of a different reporter gene; results not shown). On the other hand, no interaction was detected between β-dystrobrevin and human dysbindin-related protein, which is also known

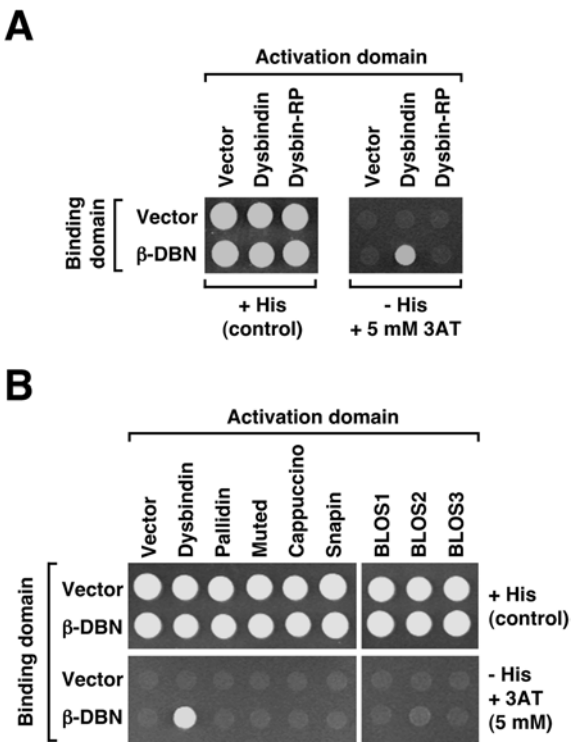

Figure 1 Interaction between human dysbindin and β-dystrobrevin in the context of the yeast two-hybrid system

(**A**) Analysis of interaction between β-dystrobrevin and dysbindin or dysbindin-related protein (Dysbin-RP). (**B**) Analysis of interaction between β-dystrobrevin (β-DBN) and the eight known subunits of BLOC-1. (**A**, **B**) Yeast cells were co-transformed with expression plasmids encoding Gal4 DNA-binding and activation domains alone (Vector) or fused in-frame to the full-length ORFs of the indicated human proteins. Double transformants were grown on minimal medium lacking leucine and tryptophan and containing histidine, suspended in distilled water at equal cell density, and then spotted on the same medium (+His) or on selective medium lacking histidine (−His) and containing 5 mM 3AT. Colony growth was examined after 3 days of culture at 30 °C.

as hypothetical protein CAB83042 or *Homo sapiens* uncharacterized hypothalamus protein HSMNP1 [12] and has occasionally been called dysbindin-2 [19] (Figure 1A). Since dysbindin is a component of BLOC-1, of which another subunit, muted, was reported to interact with β-dystrobrevin as well [13], we tested for binding between β-dystrobrevin and each of the eight known BLOC-1 subunits. As shown in Figure 1(B), dysbindin was the only BLOC-1 subunit that displayed significant dystrobrevin-binding activity in the yeast two-hybrid system under 'high-stringency' conditions (i.e. as assayed by growth in the absence of histidine and presence of 5 mM 3AT). Weak interactions between β-dystrobrevin and either muted or BLOS2 were evidenced by growth of co-transformed yeast in the absence of histidine and 3AT (results not shown).

We next sought to map the regions of dysbindin and β-dystrobrevin that are sufficient for the observed binding activity. As noted before [12,35,36], both proteins contain a tandem of two segments with significant propensity to adopt coiled-coil structures (Figure 2A). Human α-dystrobrevin, which has also been reported to interact with dysbindin [12], contains a tandem of two coiled-coil-forming segments highly similar to those of β-dystrobrevin as well as a third coiled-coil-forming region close to its C-terminus (Figure 2A). Consistent with an existing nomenclature, we refer to the two coiled-coil-forming segments conserved in the dystrobrevins as H1 and H2 [37,38], and to the region comprising both segments in tandem as CC [1,36]. In the case of

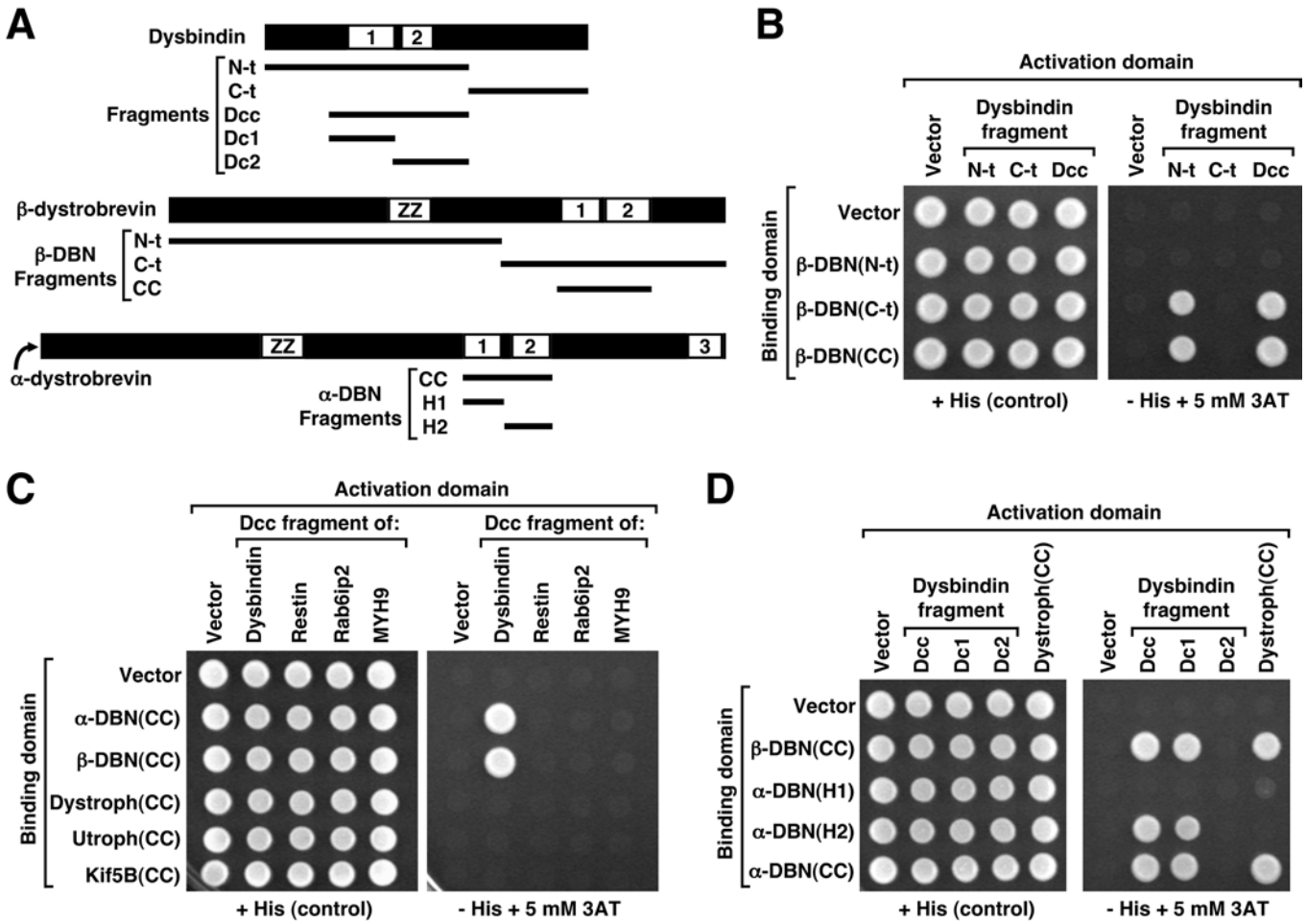

Figure 2 Mapping of regions involved in the interaction between dysbindin and the dystrobrevins using the yeast two-hybrid system

(**A**) Schematic representation of the predicted domain organizations of dysbindin and the α- and β-dystrobrevins (DBNs), as well as of fragments used for mapping experiments. Coiled-coil-forming domains in each protein are denoted with numbers on a white background; notice that there is no significant identity between the coiled-coil-forming regions of dysbindin and those of the dystrobrevins. Both dystrobrevins also contain a ZZ-type zinc finger. (**B**–**D**) Yeast cells were co-transformed with expression plasmids encoding Gal4 DNA-binding and activation domains alone (vector) or fused in-frame to the indicated human protein segments. The Dystroph(CC), Utroph(CC) and Kif5B(CC) constructs contain segments of dystrophin, utrophin and kinesin heavy chain Kif5B respectively, which display identity to the CC region of the dystrobrevins. Likewise, the 'Dcc fragments' of restin, Rab6ip2 and MYH9 are related to the Dcc region of dysbindin. Double transformants were spotted on minimal medium lacking leucine and tryptophan and containing histidine (+His) or lacking histidine and containing 5 mM 3AT (−His + 5 mM 3AT). Colony growth was examined by visual inspection after 3 days of culture at 30 °C.

the dysbindin molecule, we hereafter use the name 'Dcc' for the dysbindin coiled-coil tandem region and 'Dc1' and 'Dc2' for fragment constructs including each separate coiled-coil-forming segment (Figure 2A). As shown in Figure 2(B), co-transformed yeast cells expressing binding domain constructs including the CC region of β-dystrobrevin, together with activation domain constructs including the Dcc segment of dysbindin, displayed vigorous growth on selective medium lacking histidine and containing 5 mM 3AT. On the other hand, yeast cells expressing the binding domain fused to the N-terminal (N-t) approximately three-fifths of β-dystrobrevin, the activation domain fused to the C-terminal (C-t) approximately one-third of dysbindin, or both, failed to grow on selective medium (Figure 2B). These results suggest that the CC region of β-dystrobrevin and the Dcc segment of dysbindin are sufficient for interaction between the two proteins.

Because we were concerned that the observed yeast two-hybrid interaction could result from non-specific formation of coiled coils, we searched for related coiled-coil-forming regions that could be used as specificity controls. It is well known that the CC region of β-dystrobrevin is conserved not only in its closest paralogue, α-dystrobrevin (96 % identical amino acids over a 94-residue overlap), but also in dystrophin, utrophin and dystrophin-related protein 2 (29, 28 and 31 % identical residues respectively) [35–37]. In addition, homology searches of the NCBI *Homo sapiens* Reference Proteins Database (29 282 sequences at the time the search was done), using the BLASTP algorithm, suggested that the CC region of β-dystrobrevin is also related to a coiled-coil-forming region within kinesin heavy chains Kif5B [26 % identity over a 93-residue overlap; E-value (expected value) = 2×10^{-6}] and Kif5A (E-value = 4×10^{-5}). Interestingly, similar searches using the Dcc region of dysbindin as a query identified at least three other human proteins bearing related coiled-coil-forming regions; namely Rab6ip2 (also known as ELKS or ERC1; E-value = 2×10^{-5}), MYH9 (E-value = 2×10^{-5}) and restin (Reed–Steinberg cell-expressed intermediate filament-associated protein, also known as CLIP-170; E-value = 2×10^{-4}). Although these 'hits' do not necessarily represent true homology [39], we considered that these protein segments would serve as appropriate controls to test the specificity of the dystrobrevin–dysbindin

interaction in the context of the yeast two-hybrid system. As shown in Figure 2(C), out of 20 interaction pairs tested among coiled-coil-forming fragments, only those comprising the CC region of α- or β-dystrobrevin and the Dcc region of dysbindin gave positive results, as determined by growth of the co-transformed cells in the absence of histidine and presence of 5 mM 3AT.

Next, we tested whether individual coiled-coil-forming regions of each protein would be sufficient for interaction. As shown in Figure 2(D), co-transformed yeast cells expressing hybrid proteins containing the first coiled-coil-forming region of dysbindin and the second such region of α-dystrobrevin were able to grow in the absence of histidine and presence of 5 mM 3AT, whereas cells expressing the Dc2 region of dysbindin and/or the H1 region of α-dystrobrevin were unable to grow under the same conditions (Figure 2D) or conditions of low stringency (results not shown). The CC region of α- or β-dystrobrevins interacted with the CC region of dystrophin (Figure 2D), as previously reported [38].

In vitro binding experiments

To examine the dystrobrevin–dysbindin interaction using an *in vitro* biochemical method, we generated recombinant GST-fusion proteins comprising the CC regions of the α- and β-dystrobrevins [GST–α-DBN(CC) and GST–β-DBN(CC) respectively] and a polyhistidine-fusion protein containing the Dcc region of dysbindin, His–Dysbin(Dcc). Our choice of using recombinant proteins containing the entire CC regions of the dystrobrevins, and not just the H2 segment, allowed us to test for their interaction with dystrophin [38] as a positive control. As negative controls we used irrelevant GST-fusion proteins, a GST fusion bearing the CC region of utrophin [GST–Utroph(CC)] and a polyhistidine-fusion protein containing the Dcc-like region of MYH9 [His–MYH9(Dcc)]. All of these recombinant proteins were soluble and relatively easy to purify in milligram amounts (results not shown). On the other hand, our attempts to obtain a GST-fusion protein comprising the full-length β-dystrobrevin were hampered by the low solubility of the recombinant protein (results not shown).

We first used a standard 'GST-pulldown' assay, in which soluble polyhistidine-fusion proteins were incubated with purified GST-fusion proteins that had been immobilized on to glutathione–Sepharose beads, and the beads were then washed and analysed for the presence of bound polyhistidine-fusion protein. Because the composition of the binding buffer might be a critical factor of the assay, we performed parallel experiments using three different binding buffers. For the sake of simplicity, we refer to them as 'Detergent-free', 'Triton X-100' and 'Tween 20' buffers. It should be noted that the presence or absence and the type of detergent were not the only differences between these buffers: for example, the Detergent-free buffer contained KCl instead of NaCl, and the Triton X-100 buffer but not the others contained sucrose and $MgCl_2$ (see the Experimental section for detailed buffer compositions). The Tween 20 buffer was identical with the one used in a previous study demonstrating biochemical interaction between the CC regions of α-dystrobrevin and dystrophin [38], while the Detergent-free and Triton X-100 buffers were chosen to allow preparation of cytosolic and solubilized membrane extracts respectively for subsequent pulldown experiments (described below). Regardless of which of these three binding buffers was used, a polyhistidine-fusion protein containing the CC region of dystrophin [His–Dystroph(CC)] bound specifically to GST–α-DBN(CC) and GST–β-DBN(CC), but not to irrelevant GST-fusion proteins or to GST–Utroph(CC) (results not shown). On the other hand, the His–MYH9(Dcc) protein displayed no significant binding to any of the GST-fusion proteins tested (Figures 3A and 3B and results not shown). Under the same conditions, the His–Dysbin(Dcc) protein containing the Dcc region of dysbindin consistently bound to GST-fusion proteins containing the CC regions

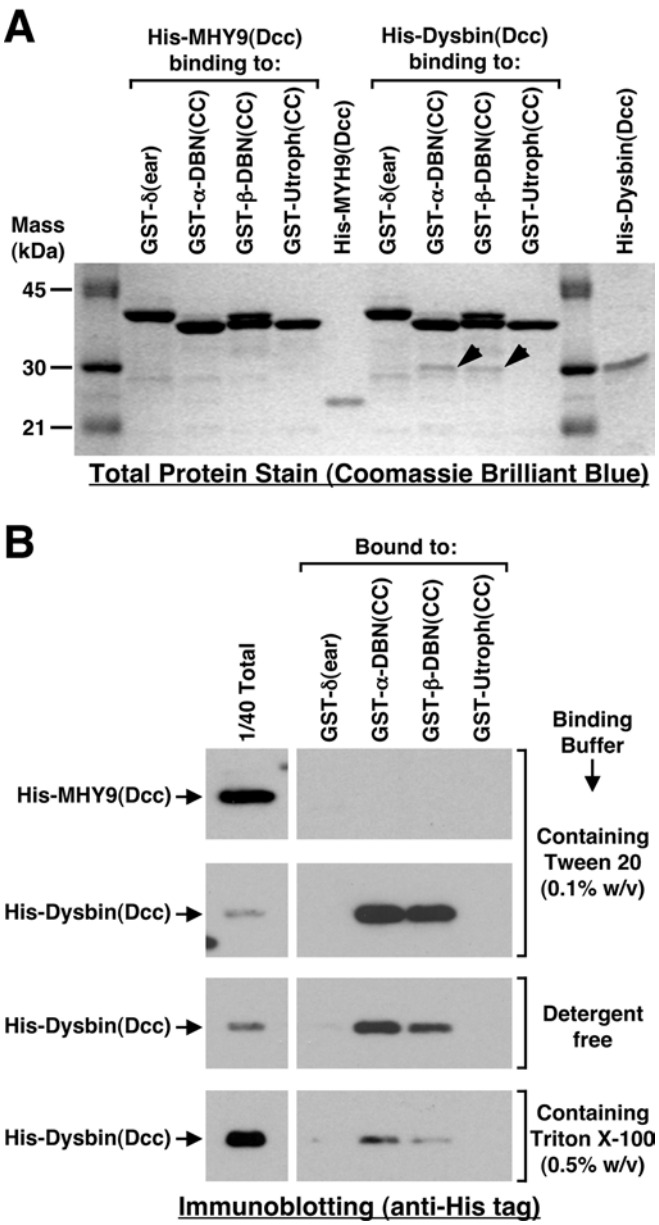

Figure 3 Interaction between recombinant proteins containing the coiled-coil-forming domains of dysbindin and the dystrobrevins

Purified GST-fusion proteins containing the coiled-coil-forming segments (CC) of human α-dystrobrevin (α-DBN), β-dystrobrevin (β-DBN) and utrophin (Utroph), as well as the irrelevant GST-δ(ear) protein, were immobilized on glutathione–Sepharose beads and incubated with purified polyhistidine-tagged-fusion proteins containing the dysbindin coiled-coil-forming region [His–Dysbin(Dcc)] or the corresponding region in MYH9 [His–MYH9(Dcc)]. Following incubation, the beads were isolated by centrifugation, washed extensively, and heated in the presence of SDS/PAGE sample buffer. Samples were analysed by SDS/PAGE followed by Coomassie Brilliant Blue staining (**A**) or immunoblotting using a monoclonal antibody to the polyhistidine tag (**B**). Arrowheads in (**A**) denote the presence of His–Dysbin(Dcc) protein associated with GST–α-DBN(CC) and GST–β-DBN(CC). In (**B**), each pair of '1/40 total' and 'Bound' digital images is derived from portions of a single immunoblot that was exposed to a film, scanned and processed under identical conditions. Notice that the His–Dysbin(Dcc) protein specifically bound to both GST–α-DBN(CC) and GST–β-DBN(CC), although the relative amounts of bound His–Dysbin(Dcc) varied depending on the composition of the binding buffer. Further details on the buffer compositions are provided in the main text.

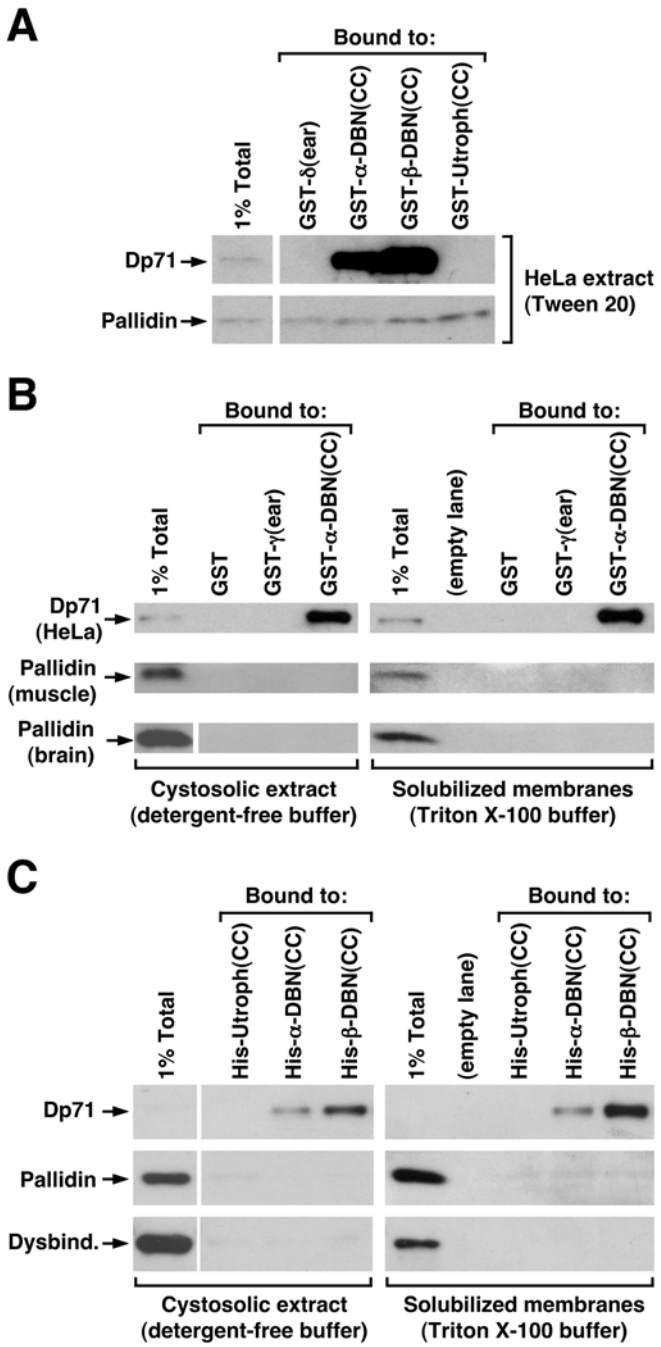

Figure 4 Affinity-pulldown binding experiments using cell-free extracts

(**A**, **B**) The indicated GST-fusion proteins were immobilized on glutathione–Sepharose beads and subsequently incubated with cell-free extracts freshly prepared from HeLa cells, mouse whole brain, or mouse quadriceps muscle, using the indicated buffers (see the text for buffer compositions and further experimental details). Following the incubation period, the beads were isolated by brief centrifugation, washed with ice-cold buffer, and then heated in the presence of SDS/PAGE sample buffer to elute the GST-fusion proteins and any associated proteins. Eluted protein samples were analysed by immunoblotting using monoclonal antibodies to dystrophin (to detect the Dp71 isoform as a positive control) or to the pallidin subunit of BLOC-1. (**C**) Polyhistidine-fusion proteins containing the S-tag sequence and the coiled-coil-forming domains (CC) of human α-dystrobrevin (α-DBN), β-dystrobrevin (β-DBN) and utrophin (Utroph) were immobilized on Protein S–agarose beads and subsequently incubated with freshly prepared cytosolic and solubilized membrane protein extracts from HeLa cells. Following incubation, the beads were recovered by centrifugation and washed. Bound proteins were eluted using SDS/PAGE sample buffer, and then analysed by immunoblotting using monoclonal antibodies to dystrophin/Dp71 and pallidin or a polyclonal antibody to dysbindin. Each image of the control lane represents 1 % of the total extract and is from the same immunoblot exposed to a film, scanned and processed under identical conditions as the images corresponding to 'Bound' material. Notice in (**C**) that the relative amounts of Dp71 bound to His–α-DBN(CC) and His–β-DBN(CC) were such that the Dp71 protein band was only visible in the '1 % Total' control lane after a significantly longer exposure (not shown).

of α- and β-dystrobrevins, but not to irrelevant GST-fusion proteins or to GST–Utroph(CC) (Figures 3A and 3B). Although the relative amounts of bound His–Dysbin(Dcc) varied depending on the composition of the binding buffer (Figure 3B), these amounts were comparable with those of bound His–Dystroph(CC) (results not shown). Therefore these results verified that the dystrobrevin–dysbindin interaction is direct and that the CC region of the dystrobrevins and the Dcc region of dysbindin are sufficient for binding *in vitro*.

Encouraged by the results obtained using purified recombinant proteins, we used the GST-pulldown assay to test whether endogenous dysbindin assembled into BLOC-1 from HeLa cells and mouse tissues was able to bind the CC regions of the dystrobrevins. To probe for the presence of BLOC-1 in the washed beads, we used a monoclonal antibody to the pallidin subunit of the complex. As a positive control of the assay, we also tested for the presence of Dp71 (a widely expressed isoform of dystrophin) in the washed beads. As shown in Figure 4(A), significant amounts of Dp71 from a HeLa cell extract prepared in Tween 20 buffer were recovered bound to the GST–α-DBN(CC) and GST–β-DBN(CC)-fusion proteins, but not to the control GST-fusion proteins, whereas pallidin was found non-specifically associated in small amounts to all GST-fusion-containing beads. Similarly, large amounts of Dp71 from HeLa cytosolic and solubilized membrane extracts specifically bound to GST–α-DBN(CC) (Figure 4B) and GST–β-DBN(CC) (results not shown), whereas no significant binding was observed for pallidin from cytosolic or solubilized membrane extracts prepared from HeLa cells (results not shown) or mouse muscle or brain (Figure 4B). It should be emphasized that these GST-pulldown experiments were carried out using the same binding buffers and washing conditions as those used for the experiments shown in Figure 3, which demonstrated binding of recombinant His–Dysbin(Dcc) to GST–α-DBN(CC) and GST–β-DBN(CC). Finally, the binding of endogenous dysbindin, which could not be directly assessed in GST-pulldown assays due to weak cross-reactivity between the anti-dysbindin antibody and the GST moiety (results not shown), was examined using a different set of pulldown experiments. Specifically, polyhistidine-fusion proteins containing the S-tag sequence and the CC regions of utrophin (as negative control) and of α- and β-dystrobrevins were immobilized on to Protein S–agarose beads, and the beads were subsequently incubated with HeLa extracts, washed and analysed by immunoblotting. As shown in Figure 4(C), again Dp71 bound robustly to the fusion proteins containing the CC regions of α- and β-dystrobrevins, and not to the control protein, whereas neither pallidin nor dysbindin interacted with any of the polyhistidine-fusion proteins (notice that Dp71 bound to the dystrobrevins was readily observed under conditions in which Dp71 was not yet detectable in the lane corresponding to 1 % Total; Figure 4C). Similar results were obtained using extracts prepared from mouse brain (results not shown).

Analysis of *in vivo* association between the dystrobrevins, dysbindin and pallidin

Although various technical reasons could be invoked to explain our failure to detect specific interaction between recombinant portions of the dystrobrevins and endogenously expressed dysbindin/BLOC-1, these negative results prompted us to re-examine the reported *in vivo* association between dysbindin and

dystrobrevins from brain and muscle [12]. We prepared detergent extracts of brain and quadriceps muscle freshly dissected from both mice and rats, following the procedure described in a previous study [12] and using basically the same homogenization buffer (herein referred to as Co-immunoprecipitation buffer; see the Experimental section for a detailed buffer composition) and variations of it in which the concentration of Triton X-100 was raised from 0.5 % to up to 2 % (w/v). In all experiments, the detergent extracts were pre-cleared with Protein A–Sepharose and/or Protein G–Sepharose to remove endogenous IgG, and then immunoprecipitated using a mouse monoclonal antibody to the dystrobrevins, an affinity-purified rabbit polyclonal antibody to dysbindin, and equal amounts of control IgG or affinity-purified rabbit antibodies to irrelevant proteins. The washed immunoprecipitates were then analysed by immunoblotting using monoclonal antibodies to the dystrobrevins and to the pallidin subunit of BLOC-1. Results from representative experiments are shown in Figure 5. As expected, the anti-dystrobrevin antibody immunoprecipitated endogenous α- and β-dystrobrevin isoforms expressed in mouse and rat brain (Figure 5A and results not shown) as well as α-dystrobrevin isoforms expressed in mouse (Figure 5B) and rat (Figure 5C) muscle. The anti-dysbindin antibody efficiently immunoprecipitated BLOC-1 from both brain and muscle, as judged by the significant amounts of the pallidin subunit specifically recovered from the dysbindin immunoprecipitates relative to the amounts detected in aliquots of the total extract (Figures 5A and 5B). On the other hand, no pallidin was detected in the dystrobrevin immunoprecipitates, and only minute amounts of dystrobrevins (< 0.1 %) were found in the dysbindin immunoprecipitates (Figures 5A–5C). Importantly, these small amounts of dystrobrevins detected in the dysbindin immunoprecipitates were comparable with those found in control immunoprecipitates obtained using irrelevant antibodies (Figures 5A and 5C), indicating non-specific association of dystrobrevins to antibody-laden Protein A–Sepharose beads. Similar results were obtained in three independent experiments using extracts prepared from mouse muscle (using 0.5 or 1 % Triton X-100), two independent experiments using extracts prepared from rat muscle (using 0.5 or 1 % Triton X-100), two experiments using mouse brain (using 1 or 2 % Triton X-100) and one experiment using rat brain (using 1 % Triton X-100).

Intersubunit interactions within BLOC-1 may interfere with the ability of dysbindin to bind dystrobrevins

Published results suggest that dysbindin within BLOC-1 interacts directly with the pallidin, snapin and muted subunits [13,24]. Here, we sought to map the regions of dysbindin involved in binding to these subunits, to test whether they overlap with the Dc1 region that binds dystrobrevins. To this end, dysbindin fragments fused to the Gal4 activation domain were assayed for interaction with full-length pallidin, snapin and muted fused to the Gal4-binding domain, using the yeast two-hybrid system. As shown in Figure 6(A), the Dc1 region of dysbindin was sufficient for interaction with pallidin and snapin, as inferred from growth of co-transformed yeast cells in medium lacking histidine and containing 5 mM 3AT. Under the same stringency conditions, the complete coiled-coil tandem region of dysbindin, Dcc, seemed to be required for binding to muted (Figure 6A), although the Dc1 region (and not Dc2) was sufficient for interaction with muted as assayed under conditions of lower stringency (results not shown). Therefore the same 69-residue segment of the dysbindin molecule that is sufficient for dystrobrevin binding is also sufficient for binding to pallidin and snapin and, together with the Dc2 region, for optimal binding to muted (see scheme in Figure 6B).

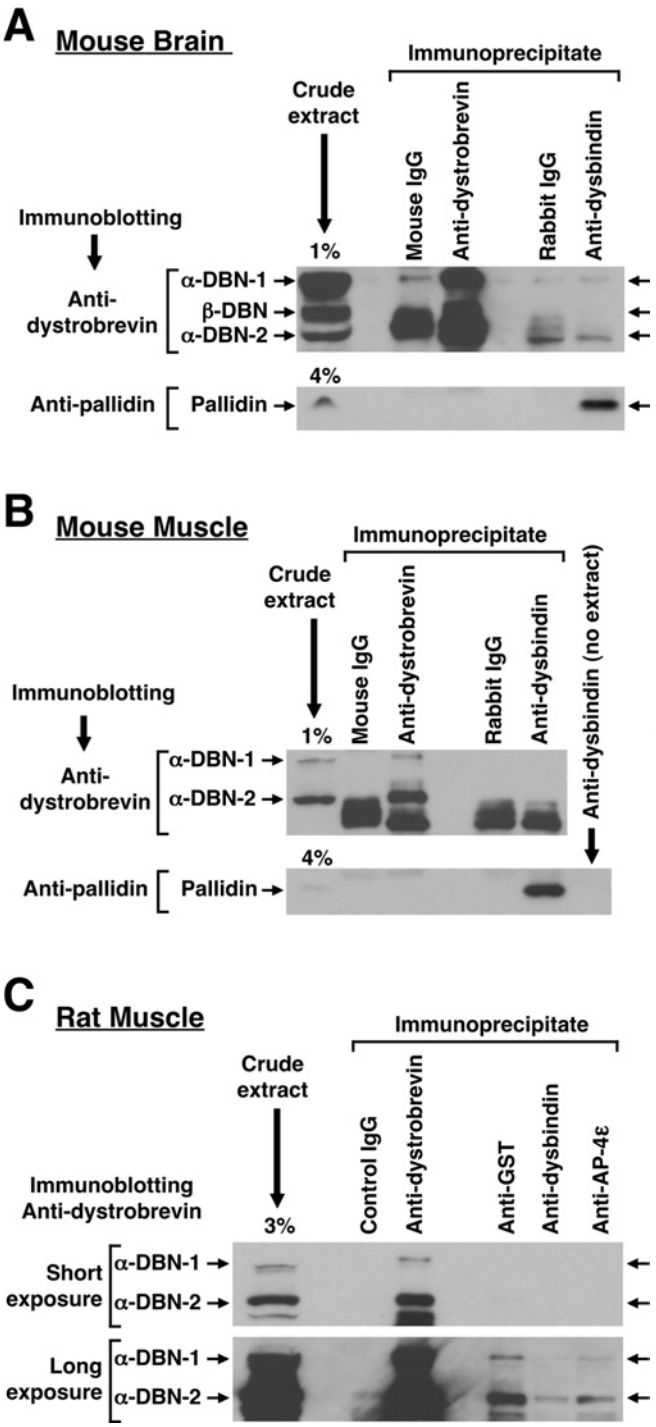

Figure 5 Co-immunoprecipitation experiments

Detergent extracts prepared from mouse brain (**A**), mouse quadriceps muscle (**B**) or rat quadriceps (**C**) were subjected to immunoprecipitation using a mouse monoclonal antibody against α- and β-dystrobrevins, a rabbit polyclonal antibody to dysbindin, and comparable amounts of the indicated control antibodies. The washed immunoprecipitates were analysed by immunoblotting using monoclonal antibodies to dystrobrevin or pallidin. Small aliquots (1–4 % as indicated) of the crude extracts used for immunoprecipitation were analysed in parallel. Notice in (**A**, **B**) that significant amounts of pallidin were specifically recovered from the sample immunoprecipitated using anti-dysbindin, and that no dystrobrevin was found in the anti-dysbindin immunoprecipitate in amounts higher than in control immunoprecipitates. Similarly, only minute amounts of α-dystrobrevin isoforms were detected in the anti-dysbindin immunoprecipitate obtained from rat quadriceps extracts, and these amounts were not higher than those of dystrobrevins non-specifically associated with immunoprecipitates obtained using irrelevant rabbit polyclonal antibodies (**C**).

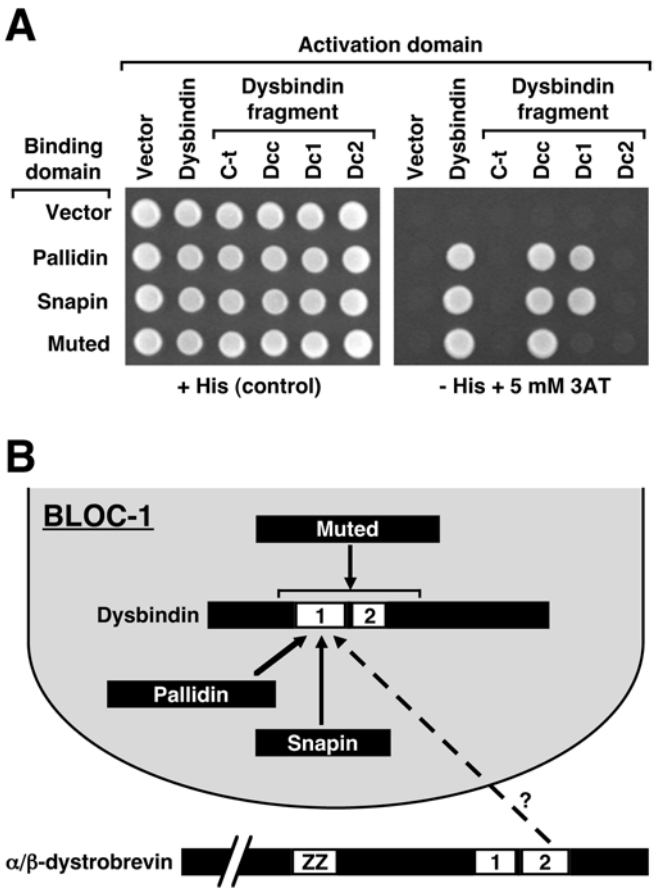

Figure 6 Mapping of dysbindin regions involved in interaction with other BLOC-1 subunits using the yeast two-hybrid system

(**A**) Yeast cells were co-transformed with expression plasmids encoding Gal4 DNA-binding and activation domains alone (vector), fused in-frame to the full-length ORFs of human dysbindin, pallidin, snapin and muted, or fused in-frame to the indicated fragments of human dysbindin. Double transformants were grown on minimal medium lacking leucine and tryptophan and containing histidine (+His), suspended in distilled water at an equal cell density, and then spotted on the same medium or on selective medium lacking histidine (−His) and containing 5 mM 3AT. Colony growth was examined after 3 days of culture at 30 °C. (**B**) Schematic representation of how the results shown in Figures 2(D), 3, 4 and 5 can be interpreted in light of the results shown in (**A**). For the sake of simplicity, only the relevant BLOC-1 subunits are shown, and the coiled-coil-forming regions of muted, pallidin and snapin are not depicted.

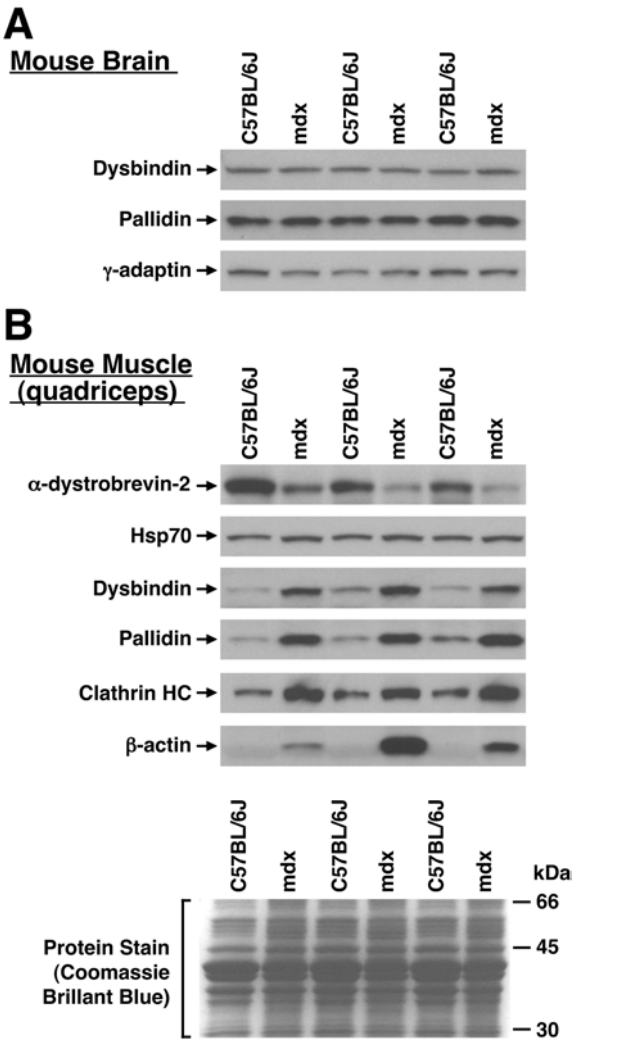

Figure 7 Immunoblot analysis of the relative contents of selected proteins in whole-tissue extracts prepared from wild-type and dystrophin-deficient mice

Extracts were prepared from brain (**A**) or quadriceps muscle (**B**) freshly dissected from 2-month-old male mice of wild-type (C57BL/6J) or dystrophin-deficient (mdx) strains (3 mice per strain). The extracts (60 μg of total protein) were analysed by SDS/PAGE, followed by immunoblotting using specific antibodies against the indicated proteins (clathrin HC, clathrin heavy chain). The lower panel in (**B**) shows a portion of a duplicate SDS/polyacrylamide gel that was stained using Coomassie Brilliant Blue.

Steady-state levels of dysbindin and other proteins in brain and muscle from dystrophin-deficient mice

Previous work had demonstrated that dysbindin protein levels are increased in muscle of dystrophin-deficient mdx mice, as compared with muscle of C57BL/6J wild-type mice, lending support to the notion that dysbindin is involved in the pathogenesis of muscular dystrophy [12]. Here, we examined whether such an increase was restricted to muscle tissue and whether it was accompanied by up-regulation of other BLOC-1 subunits. To this end, whole-tissue extracts prepared from brain and quadriceps muscle dissected from wild-type and mdx mice were analysed by immunoblotting. Because the levels of specific proteins might vary according to the gender and age of the animals, we chose to restrict our analysis to 2-month-old male mice. Total protein concentration was determined in all extracts, and normalized prior to SDS/PAGE fractionation and immunoblotting. As shown in Figure 7(A), the steady-state protein levels of both dysbindin and pallidin were virtually identical in brains from wild-type and mdx mice. As expected, the level of α-dystrobrevin isoform 2 was significantly reduced in muscle from mdx mice, whereas that of the housekeeping Hsp70 (heat-shock protein 70) protein was either unaltered or moderately increased (Figure 7B). In agreement with previous work [12], the steady-state level of dysbindin in mdx muscle extracts was increased to approx. 4 times that of wild-type muscle (two-tail unpaired Student's t test, $P < 0.01$; Figure 7B). Interestingly, the level of pallidin was increased in mdx muscle to a similar extent ($P < 0.01$; Figure 7B) and the same was observed for the snapin subunit of the same complex (results not shown). Hence, the relative content of BLOC-1, not just dysbindin, was higher in muscle extracts from mdx mice. Surprisingly, we also noted that the levels of several other proteins, which we tested as 'loading controls,' were likewise increased in mdx muscle extracts, despite comparable total protein loading as judged by Coomassie Brilliant Blue staining (Figure 7B, bottom panel). These proteins included clathrin heavy chain ($P = 0.013$;

Figure 7B) as well as α- and γ-adaptins, α-tubulin and Rab11 (results not shown). We also probed the immunoblots with a monoclonal antibody to 'non-muscle' β-actin, the expression of which is significantly down-regulated as myoblasts differentiate into myotubes (see, for example, [40,41]). Strikingly, β-actin was readily detected in muscle extracts from mdx mice, under conditions in which the protein was not detectable in wild-type muscle (Figure 7B). These results suggest that the relative protein levels of dysbindin and other BLOC-1 subunits are increased in muscle from mdx mice, but that such increases do not necessarily imply a role in the pathogenesis of muscular dystrophy as they might be secondary to differences in cell type composition and/or cell differentiation stage between mdx and wild-type mouse skeletal muscle [42].

Apparently normal muscle histology and function in BLOC-1-deficient mice

As an alternative approach to test whether BLOC-1 is functionally linked to the DGC and plays a significant role in the pathogenesis of muscular dystrophy, we analysed homozygous pallid mice for signs of muscle pathology. Pallid mice carry a nonsense mutation in the pallidin-encoding gene [25] and display no detectable pallidin protein as well as drastically reduced levels of all of the remaining BLOC-1 subunits – including dysbindin – due to compromised complex stability [13,24–27]. Mice of 4 months and over 1 year of age were analysed. First, muscle strength was examined by means of the wire-hanging test [33]. In this test, wild-type mice can hang for 1 min at a time easily, whereas mice with muscle disease (e.g. mdx mice) have difficulty with this task [33,43]. None of the homozygous pallid mice demonstrated any limitation in their ability to hang during 1 min periods (results not shown). Secondly, muscle sections were analysed by both standard histological and immunohistochemical methods. No signs of muscle necrosis, inflammation or repair were detected in any of the muscle types examined (results not shown). Finally, muscle sections were stained using monoclonal antibodies to dystrophin and the dystrobrevins (as well as to laminin, as a control). As exemplified by the representative images shown in Figure 8, muscle sections derived from pallid mice displayed the normal characteristic distribution of dystrophin and α-dystrobrevin. These results suggest that BLOC-1 function is dispensable for normal assembly and localization of the DGC in mouse muscle, and that BLOC-1 deficiency does not lead to any of the main manifestations observed in mouse models of muscular dystrophy, such as the mdx [42] and α-dystrobrevin-deficient [5] mice.

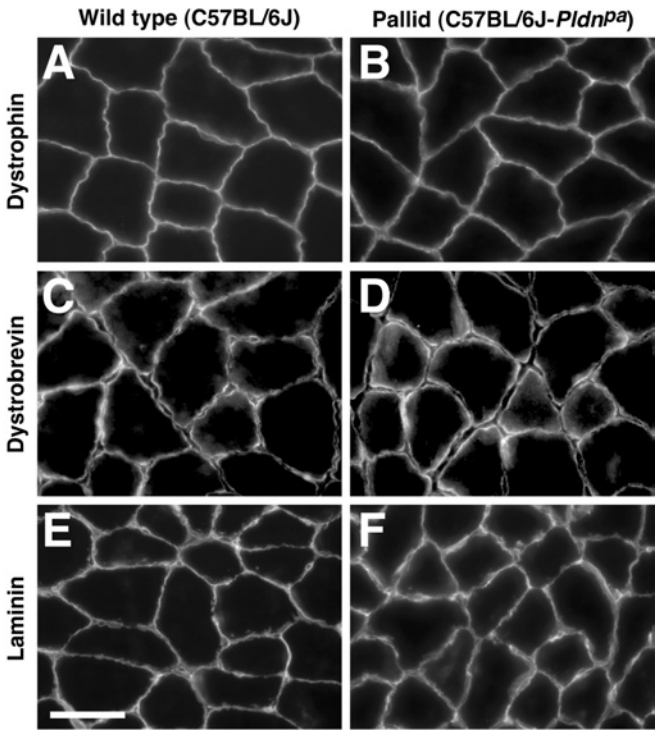

Figure 8 Immunohistochemical analyses of muscle sections from wild-type and BLOC-1-deficient (pallid) mice

Sections of quadriceps dissected from 4-month-old female mice of the indicated strains were stained using antibodies to dystrophin (**A**, **B**), dystrobrevin (**C**, **D**) and laminin (**E**, **F**) followed by appropriate secondary antibodies conjugated with Texas Red (**A**, **B**) or fluorescein (**C**–**F**). Scale bar, 50 μm.

DISCUSSION

The goal of the present study was to further investigate the previously reported dystrobrevin–dysbindin interaction [12] as an approach to gain insights into the molecular function of the dysbindin-containing protein complex, BLOC-1. As mentioned in the Introduction section, such a physical interaction is potentially relevant to the roles proposed for dysbindin (and, by extension, BLOC-1) in the pathogenesis of muscular dystrophy, schizophrenia and HPS. We studied the interaction by means of the yeast two-hybrid system and affinity-pulldown assays using recombinant protein fragments, two approaches in which binding was assessed in the context of dysbindin not assembled into BLOC-1. We performed additional affinity-pulldown assays, and co-immunoprecipitation experiments, using endogenous BLOC-1 from muscle and brain tissues as well as from cultured HeLa cells. The results appeared contradictory at first examination: while the dystrobrevin–dysbindin interaction was readily detected and deemed specific in the context of unassembled dysbindin, we were consistently unable to detect it in the context of native BLOC-1.

We report that the *in vitro* interaction between unassembled dysbindin and the dystrobrevins involves coiled-coil-forming regions of both proteins. Specifically, the first coiled-coil-forming domain of dysbindin ('Dc1' region, 69 amino acid residues) and the second coiled-coil-forming domain of α-dystrobrevin ('H2' region, 54 residues) were sufficient for binding in the yeast two-hybrid system under high-stringency conditions, and coiled-coil-forming segments including each of them ('Dcc' and 'CC' regions respectively) were sufficient for direct binding as determined by *in vitro* pulldown assays. Our results demonstrating a dystrobrevin-binding site within the coiled-coil-forming domain of dysbindin are consistent with published results on the apparent lack of dystrobrevin-binding activity displayed by the product of the mouse sandy (*Dtnbp1*^{sdy}) allele [13], which carries an in-frame deletion encompassing the last 22 residues of the Dc1 region as well as part of Dc2. It is also consistent with the inability of dystrobrevin to interact with dysbindin-related protein, which despite its overall similarity to dysbindin lacks a region homologous with the Dc1 domain. On the other hand, our results demonstrating a dysbindin-binding site within the H2 coiled-coil-forming region of the dystrobrevins are at variance with previous work from another group, which had instead proposed that dysbindin binds to the N-terminal region of the dystrobrevins [12]. The reasons for this apparent inconsistency are unclear, although differences in experimental approaches could be invoked. Nevertheless, our results obtained using unassembled dysbindin (i.e. in the yeast two-hybrid system or as a recombinant protein fragment) lend

support to the idea that the dysbindin–dystrobrevin interaction may be specific [12].

On the other hand, recombinant fusion proteins bearing the CC region of either α- or β-dystrobrevin were unable to bind native BLOC-1 extracted from three different sources (HeLa cells, mouse quadriceps and mouse whole brain) using three different buffers (Tween 20, Triton X-100 and Detergent-free buffers). Under these conditions, these fusion proteins seemed to be correctly folded and active, as judged from their ability to bind a recombinant form of the Dcc region of dysbindin as well as recombinant and native forms of dystrophin/Dp71. Several reasons could be invoked to explain these results. For example, it could be that other parts of the dystrobrevins besides their CC region are required for high-affinity binding to native BLOC-1. Unfortunately, we have been unable to obtain full-length dystrobrevins in soluble recombinant form to test this idea experimentally. Another possibility is that BLOC-1 might bind dystrobrevins only in an 'active' conformation that could be absent or represent a minor fraction of extracted BLOC-1. Yet another possibility is that dysbindin could interact with the dystrobrevins only when not assembled into BLOC-1, although it should be mentioned that our attempts to detect binding of recombinant dystrobrevin fragments to endogenous dysbindin, using BLOC-1-expressing cells and tissues (Figure 4C and results not shown) as well as pallid mutant brain samples containing dysbindin not assembled into BLOC-1 (results not shown), gave in all cases negative results. While these and other considerations preclude drawing definitive conclusions solely from these affinity-pull-down experiments, these results prompted us to reinvestigate the association between dysbindin and dystrobrevins *in vivo*. In contrast with a previous report [12], we found no evidence of specific association between these proteins in muscle or brain from rodents. Specifically, immunoprecipitation of endogenous dysbindin using a well-characterized, affinity-purified rabbit polyclonal antibody [24] under mild non-denaturing conditions resulted in robust co-immunoprecipitation of the pallidin protein, as expected from association of dysbindin and pallidin into BLOC-1 [13,24], but not of α- or β-dystrobrevins. Similar results were obtained on immunoprecipitation of BLOC-1 using an antibody to the BLOS3 subunit (results not shown), which like the anti-dysbindin antibody immunoprecipitates native BLOC-1 with high efficiency [24]. Although we did detect small amounts of dystrobrevins associated with the anti-dysbindin immunoprecipitates, comparable amounts were also recovered from control immunoprecipitates obtained using irrelevant control antibodies. Therefore, in our hands, the apparent association of dystrobrevin with anti-dysbindin immunoprecipitates was deemed to be non-specific.

How can we reconcile our results obtained using isolated dysbindin with those obtained using BLOC-1? A possible explanation stems from our mapping of binding interfaces within the dysbindin molecule. The results reported herein suggest that the same Dc1 region of dysbindin that is sufficient for dystrobrevin binding *in vitro* is also sufficient for binding to the BLOC-1 subunits pallidin and snapin, and contains at least part of the binding site for the muted subunit of the same complex. Because these results were obtained by testing each interaction pair in the yeast two-hybrid system, determination of whether the Dc1 region of dysbindin can bind pallidin, snapin and muted simultaneously must await future biochemical or crystallographic work. Nevertheless, one can speculate that intersubunit interactions within BLOC-1 may render dysbindin unable to bind dystrobrevins *in vivo*. Along these lines, it seems unlikely that dysbindin can engage in simultaneous interactions with all of pallidin, snapin, muted and dystrobrevin; although coiled-coil structures comprising five α-helices have been described [44], they are far less common than coiled-coils formed by two to four helices [45].

Our experiments using mutant mouse strains also argue against the notion that BLOC-1 is directly involved in the pathogenesis of muscular dystrophy. First, although the relative protein content of dysbindin and other BLOC-1 subunits was found elevated in whole-tissue extracts from muscle of mdx mice, we also observed increased levels of several other cellular proteins not necessarily linked to DGC function and detected 'non-muscle' β-actin in mdx muscle extracts. While these observations do not disprove that dysbindin/BLOC-1 might be specifically up-regulated as a consequence of disruption of the DGC, the alternative view is that such increases in protein levels might be secondary to changes in the cellular composition of mdx muscle, for example due to a relative expansion in the population of myoblasts, muscle stem cells, fibroblasts or immune cells. Secondly, BLOC-1-deficient mice of the pallid mutant strain displayed apparently normal muscle strength and no signs of increased muscle necrosis, inflammation or regeneration. Finally, the characteristic steady-state distribution of dystrophin and α-dystrobrevin was unaffected in pallid mice.

In conclusion, the results described in the present paper lead us to propose that BLOC-1 is not a dystrobrevin-binding factor implicated in the pathogenesis of muscular dystrophy. It will be important to ascertain whether a pool of biologically active dysbindin not assembled into BLOC-1 may exist, although so far we have been unable to detect biochemically such a pool in normal tissues. Future work will be required to address this point.

We thank Jane Wen and Benjamin Wu for excellent technical assistance. We also thank Cristina A. Ghiani, Irina Kramerova and Santiago M. Di Pietro (David Geffen School of Medicine, UCLA) for critical reading of this paper. This work was supported in part by National Institutes of Health grants HL068117 (to E. C. D.) and AR046911 (to M. J. S.).

REFERENCES

1 Blake, D. J., Weir, A., Newey, S. E. and Davies, K. E. (2002) Function and genetics of dystrophin and dystrophin-related proteins in muscle. Physiol. Rev. **82**, 291–329
2 Albrecht, D. E. and Froehner, S. C. (2002) Syntrophins and dystrobrevins: defining the dystrophin scaffold at synapses. Neurosignals **11**, 123–129
3 Durbeej, M. and Campbell, K. P. (2002) Muscular dystrophies involving the dystrophin–glycoprotein complex: an overview of current mouse models. Curr. Opin. Genet. Dev. **12**, 349–361
4 Blake, D. J. (2002) Dystrobrevin dynamics in muscle-cell signaling: a possible target for therapeutic intervention in Duchenne muscular dystrophy? Neuromuscul. Disord. **12**, S110–S117
5 Grady, R. M., Grange, R. W., Lau, K. S., Maimone, M. M., Nichol, M. C., Stull, J. T. and Sanes, J. R. (1999) Role for α-dystrobrevin in the pathogenesis of dystrophin-dependent muscular dystrophies. Nat. Cell Biol. **1**, 215–220
6 Grady, R. M., Zhou, H., Cunningham, J. M., Henry, M. D., Campbell, K. P. and Sanes, J. R. (2000) Maturation and maintenance of the neuromuscular synapse: genetic evidence for roles of the dystrophin–glycoprotein complex. Neuron **25**, 279–293
7 Blake, D. J., Hawkes, R., Benson, M. A. and Beesley, P. W. (1999) Different dystrophin-like complexes are expressed in neurons and glia. J. Cell Biol. **147**, 645–657
8 Loh, N. Y., Newey, S. E., Davies, K. E. and Blake, D. J. (2000) Assembly of multiple dystrobrevin-containing complexes in the kidney. J. Cell Sci. **113**, 2715–2724
9 Loh, N. Y., Nebenius-Oosthuizen, D., Blake, D. J., Smith, A. J. H. and Davies, K. E. (2001) Role of β-dystrobrevin in nonmuscle dystrophin-associated protein complex-like complexes in kidney and liver. Mol. Cell. Biol. **21**, 7442–7448
10 Macioce, P., Gambara, G., Bernassola, M., Gaddini, L., Torreri, P., Macchia, G., Ramoni, C., Ceccarini, M. and Petrucci, T. C. (2003) β-Dystrobrevin interacts directly with kinesin heavy chain in brain. J. Cell Sci. **116**, 4847–4856
11 Albrecht, D. E. and Froechner, S. C. (2004) DAMAGE, a novel α-dystrobrevin-associated MAGE protein in dystrophin complexes. J. Biol. Chem. **279**, 7014–7023
12 Benson, M. A., Newey, S. E., Martin-Rendon, E., Hawkes, R. and Blake, D. J. (2001) Dysbindin, a novel coiled-coil-containing protein that interacts with the dystrobrevins in muscle and brain. J. Biol. Chem. **276**, 24232–24241

13 Li, W., Zhang, Q., Oiso, N., Novak, E. K., Gautam, R., O'Brien, E. P., Tinsley, C. L., Blake, D. J., Spritz, R. A., Copeland, N. G. et al. (2003) Hermansky–Pudlak syndrome type 7 (HPS-7) results from mutant dysbindin, a member of biogenesis of lysosome-related organelles complex 1 (BLOC-1). Nat. Genet. **35**, 84–89
14 Kendler, K. S. (2004) Schizophrenia genetics and dysbindin: a corner turned? Am. J. Psychiatry **161**, 1533–1536
15 Harrison, P. J. and Weinberger, D. R. (2005) Schizophrenia genes, gene expression, and neuropathology: on the matter of their convergence. Mol. Psychiatry **10**, 40–68
16 Williams, N. M., O'Donovan, M. C. and Owen, M. J. (2005) Is the dysbindin gene (*DTNBP1*) a susceptibility gene for schizophrenia? Schizophr. Bull. **31**, 800–805
17 Weickert, C. S., Straub, R. E., McClintock, B. W., Matsumoto, M., Hashimoto, R., Hyde, T. M., Herman, M. M., Weinberger, D. R. and Kleinman, J. E. (2004) Human dysbindin (*DTNBP1*) gene expression in normal brain and in schizophrenic prefrontal cortex and midbrain. Arch. Gen. Psychiatry **61**, 544–555
18 Bray, N. J., Preece, A., Williams, N. M., Moskvina, V., Buckland, P. R., Owen, M. J. and O'Donovan, M. C. (2005) Haplotypes at the dystrobrevin binding protein 1 (*DTNBP1*) gene locus mediate risk for schizophrenia through reduced *DTNBP1* expression. Hum. Mol. Genet. **14**, 1947–1954
19 Talbot, K., Eidem, W. L., Tinsley, C. L., Benson, M. A., Thompson, E. W., Smith, R. J., Hahn, C.-G., Siegel, S. J., Trojanowski, J. Q., Gur, R. E. et al. (2004) Dysbindin-1 is reduced in intrinsic, glutamatergic terminals of the hippocampal formation in schizophrenia. J. Clin. Invest. **113**, 1353–1363
20 Numakawa, T., Yagasaki, Y., Ishimoto, T., Okada, T., Suzuki, T., Iwata, N., Ozaki, N., Taguchi, T., Tatsumi, M., Kamijima, K. et al. (2004) Evidence of novel neuronal functions of dysbindin, a susceptibility gene for schizophrenia. Hum. Mol. Genet. **13**, 1699–1708
21 Li, W., Rusiniak, M. E., Chintala, S., Gautam, R., Novak, E. K. and Swank, R. T. (2004) Murine Hermansky–Pudlak syndrome genes: regulators of lysosome-related organelles. BioEssays **26**, 616–628
22 Bonifacino, J. S. (2004) Insights into the biogenesis of lysosome-related organelles from the study of the Hermansky–Pudlak syndrome. Ann. N.Y. Acad. Sci. **1038**, 103–114
23 Di Pietro, S. M. and Dell'Angelica, E. C. (2005) The cell biology of Hermansky–Pudlak syndrome: recent advances. Traffic **6**, 525–533
24 Starcevic, M. and Dell'Angelica, E. C. (2004) Identification of snapin and three novel proteins (BLOS1, BLOS2 and BLOS3/reduced pigmentation) as subunits of biogenesis of lysosome-related organelles complex-1 (BLOC-1). J. Biol. Chem. **279**, 28393–28401
25 Huang, L., Kuo, Y.-M. and Gitschier, J. (1999) The pallid gene encodes a novel, syntaxin 13-interacting protein involved in platelet storage pool deficiency. Nat. Genet. **23**, 329–332
26 Falcón-Pérez, J. M., Starcevic, M., Gautam, R. and Dell'Angelica, E. C. (2002) BLOC-1, a novel complex containing the pallidin and muted proteins involved in the biogenesis of melanosomes and platelet dense granules. J. Biol. Chem. **277**, 28191–28199
27 Moriyama, K. and Bonifacino, J. S. (2002) Pallidin is a component of a multi-protein complex involved in the biogenesis of lysosome-related organelles. Traffic **3**, 666–677
28 Zhang, Q., Li, W., Novak, E. K., Karim, A., Mishra, V. S., Kingsmore, S. F., Roe, B. A., Suzuki, T. and Swank, R. T. (2002) The gene for the muted (*mu*) mouse, a model for Hermansky–Pudlak syndrome, defines a novel protein which regulates vesicle trafficking. Hum. Mol. Genet. **11**, 697–706
29 Ciciotte, S. L., Gwynn, B., Moriyama, K., Huizing, M., Gahl, W. A., Bonifacino, J. S. and Peters, L. L. (2003) Cappuccino, a mouse model of Hermansky–Pudlak syndrome, encodes a novel protein that is part of the pallidin-muted complex (BLOC-1). Blood **101**, 4402–4407
30 Gwynn, B., Martina, J. A., Bonifacino, J. S., Sviderskaya, E. V., Lamoreux, M. L., Bennett, D. C., Moriyama, K., Huizing, M., Helip-Wooley, A., Gahl, W. A. et al. (2004) Reduced pigmentation (*rp*), a mouse model of Hermansky–Pudlak syndrome, encodes a novel component of the BLOC-1 complex. Blood **104**, 3181–3189
31 Nazarian, R., Falcón-Pérez, J. M. and Dell'Angelica, E. C. (2003) Biogenesis of lysosome-related organelles complex 3 (BLOC-3): a complex containing the Hermansky–Pudlak syndrome (HPS) proteins HPS1 and HPS4. Proc. Natl. Acad. Sci. U.S.A. **100**, 8770–8775
31a Bradford, M. M. (1976) A rapid and sensitive method for quantitation of microgram quantities of protein utilizing the principle of protein-dye binding. Anal. Biochem. **72**, 248–254
31b Laemmli, U. K. (1970) Cleavage of structural proteins during the assembly of the head of bacteriophage T4. Nature (London) **227**, 680–685
32 Dell'Angelica, E. C., Mullins, C. and Bonifacino, J. S. (1999) AP-4, a novel protein complex related to clathrin adaptors. J. Biol. Chem. **274**, 7278–7285
33 Gomez, C. M., Maselli, R., Gundeck, J. E., Chao, M., Day, J. W., Tamamizu, S., Lasalde, J. A., McNamee, M. and Wollmann, R. L. (1997) Slow-channel transgenic mice: a model of postsynaptic organellar degeneration at the neuromuscular junction. J. Neurosci. **17**, 4170–4179
34 Kamerova, I., Kudryashova, E., Tidball, J. G. and Spencer, M. J. (2004) Null mutation of calpain 3 (p94) in mice causes abnormal sarcomere formation *in vivo* and *in vitro*. Hum. Mol. Genet. **13**, 1373–1388
35 Peters, M. F., O'Brien, K. F., Sadoulet-Puccio, H. M., Kunkel, L. M., Adams, M. E. and Froehner, S. C. (1997) β-Dystrobrevin, a new member of the dystrophin family. J. Biol. Chem. **272**, 31561–31569
36 Blake, D. J., Nawrotzki, R., Loh, N. Y., Górecki, D. C. and Davies, K. E. (1998) β-Dystrobrevin, a member of the dystrophin-related protein family. Proc. Natl. Acad. Sci. U.S.A. **95**, 241–246
37 Blake, D. J., Tinsley, J. M., Davies, K. E., Knight, A. E., Winder, S. J. and Kendrick-Jones, J. (1995) Coiled-coil regions in the carboxy-terminal domains of dystrophin and related proteins: potentials for protein–protein interactions. Trends Biochem. Sci. **20**, 133–135
38 Sadoulet-Puccio, H. M., Rajala, M. and Kunkel, L. M. (1997) Dystrobrevin and dystrophin: an interaction through coiled-coil motifs. Proc. Natl. Acad. Sci. U.S.A. **94**, 12413–12418
39 Jones, D. T. and Swindells, M. B. (2002) Getting the most from PSI-BLAST. Trends Biochem. Sci. **27**, 161–164
40 Shani, M., Zevin-Sonkin, D., Saxel, O., Carmon, Y., Katcoff, D., Nudel, U. and Yaffe, D. (1981) The correlation between the synthesis of skeletal muscle actin, myosin heavy chain, and myosin light chain and the accumulation of corresponding mRNA sequences during myogenesis. Dev. Biol. **86**, 483–492
41 Kislinger, T., Gramolini, A. O., Pan, Y., Rahman, K., MacLennan, D. H. and Emili, A. (2005) Proteome dynamics during C2C12 myoblast differentiation. Mol. Cell. Proteomics **4**, 887–901
42 Bulfield, G., Siller, W. G., Wight, P. A. L. and Moore, K. J. (1984) X chromosome-linked muscular dystrophy (*mdx*) in the mouse. Proc. Natl. Acad. Sci. U.S.A. **81**, 1189–1192
43 Spencer, M. J., Marino, M. W. and Winckler, W. M. (2000) Altered pathological progression of diaphragm and quadriceps muscle in TNF-deficient, dystrophin-deficient mice. Neuromuscul. Disord. **10**, 612–619
44 Malashkevich, V. N., Kammerer, R. A., Efimov, V. P., Schulthess, T. and Engel, J. (1996) The crystal structure of a five-stranded coiled coil in COMP: a prototype ion channel? Science **274**, 761–765
45 Burkhard, P., Stetefeld, J. and Strelkov, S. V. (2001) Coiled coils: a highly versatile protein folding motif. Trends Cell Biol. **11**, 82–88

Received 12 December 2005/11 January 2006; accepted 1 February 2006
Published as BJ Immediate Publication 1 February 2006, doi:10.1042/BJ20051965